JOURNAL OF GEOPHYSICAL RESEARCH, VOL. 112, B03S05, doi:10.1029/2006JB004465, 2007

Seismically active wedge structure beneath the Coalinga anticline, San Joaquin basin, California

Chris A. Guzofski,[1,2] John H. Shaw,[1] Guoqing Lin,[3] and Peter M. Shearer[3]

Received 24 April 2006; revised 27 October 2006; accepted 11 November 2006; published 29 March 2007.

[1] We define the subsurface geometry, kinematics, and seismotectonics of the Coalinga anticline in the San Joaquin basin, central California. Using seismic reflection data and quantitative fault-related folding techniques, we present a model of the Coalinga anticline that demonstrates that the structure is composed of a stack of imbricated structural wedges, related to two major fault ramps at depth, the deepest of which ruptured during the 1983 Coalinga (M_w = 6.5) earthquake. Because of the lack of basinward deformation and the observed fold shapes, these ramps are interpreted to sole to a common upper detachment, which acts as a back thrust, forming a structural wedge. This back-thrust system generates the surface expression of the Coalinga anticline and extends to the surface as the Waltham Canyon fault and a series of related east dipping thrusts. This structural analysis helps reconcile the longstanding conflict between the southwest dipping preferred nodal plane of the 1983 main shock and the western vergence of the surface anticline. Furthermore, the seismic reflection data and our model suggest that two potentially seismogenic ramps and a major back thrust underlie the fold, rather than the single fault which has been inferred in previous studies. Using a relocated earthquake catalog, we document the three-dimensional distribution of earthquakes over a 22 year period relative to both the main fault which ruptured in the 1983 event and within the structural wedge. This analysis indicates that the majority of moment release following the 1983 event occurred within the wedge itself, compatible with a model of wedge emplacement.

Citation: Guzofski, C. A., J. H. Shaw, G. Lin, and P. M. Shearer (2007), Seismically active wedge structure beneath the Coalinga anticline, San Joaquin basin, California, *J. Geophys. Res.*, *112*, B03S05, doi:10.1029/2006JB004465.

1. Introduction

[2] The 1983 Coalinga (M_w = 6.5) earthquake provided one of the clearest examples of coseismic rupture of a segmented blind-thrust system that is manifest at the surface as a series of en echelon anticlines (Figure 1) [*Stein and Ekström*, 1992]. This earthquake lacked any surface rupture, but had an uplift signature associated with the anticline, arguing for a direct relationship between blind-thrust faulting, folding, and surface deformation [*Stein and King*, 1984; *Namson and Davis*, 1988; *Meltzer*, 1989; *Stein and Ekström*, 1992]. The lack of surface rupture from this event, however, makes direct observation of the causative fault geometry impossible, requiring the reliance instead on geodetic modeling and seismologic techniques to determine the structural characteristics of the fault. Proper definition of the geometry and kinematics of this fault and associated folds is critical to our understanding of blind-thrust earthquakes processes and important because this structure is often used as a geodynamic model for the subsurface deformation along the entire boundary of the Great Valley [*Dickinson*, 2002].

[3] For these reasons, the secondary coseismic and postseismic earthquakes within the core of the Coalinga anticline have been used in a broad range of studies to understand the brittle deformation associated with blind-thrust structures and fault-related fold growth [*Hill*, 1984; *Stein and King*, 1984; *Michael*, 1987; *Eaton*, 1990; *Eberhart-Phillips and Reasenberg*, 1990; *McGarr et al.*, 1990; *Stein and Ekström*, 1992; *Lin and Stein*, 2004]. Mechanical forward models of fault-related folds demonstrate that hanging wall brittle deformation is significantly impacted by both the geometry and strength of the master thrust fault, as well as the hanging wall structure [*Strayer and Suppe*, 2002]. Kinematically based structural models [*Shaw et al.*, 2005] provide a method by which to predict fault geometries and hanging wall structure, and can be used to make predictions of patterns of faulting and folding strains which may be associated with secondary seismicity [*Shaw and Suppe*, 1994].

[4] To gain further insights into the mechanisms of structural wedging and to improve our understanding of the seismic hazard associated with blind-thrust faults, related anticlines, and basin edge deformation in the San Joaquin,

[1]Department of Earth and Planetary Sciences, Harvard University, Cambridge, Massachusetts, USA.
[2]Now at Chevron ETC, Houston, Texas, USA.
[3]Institute of Geophysics and Planetary Physics, Scripps Institution of Oceanography, University of California, San Diego, La Jolla, California, USA.

0148-0227/07/2006JB004465$09.00

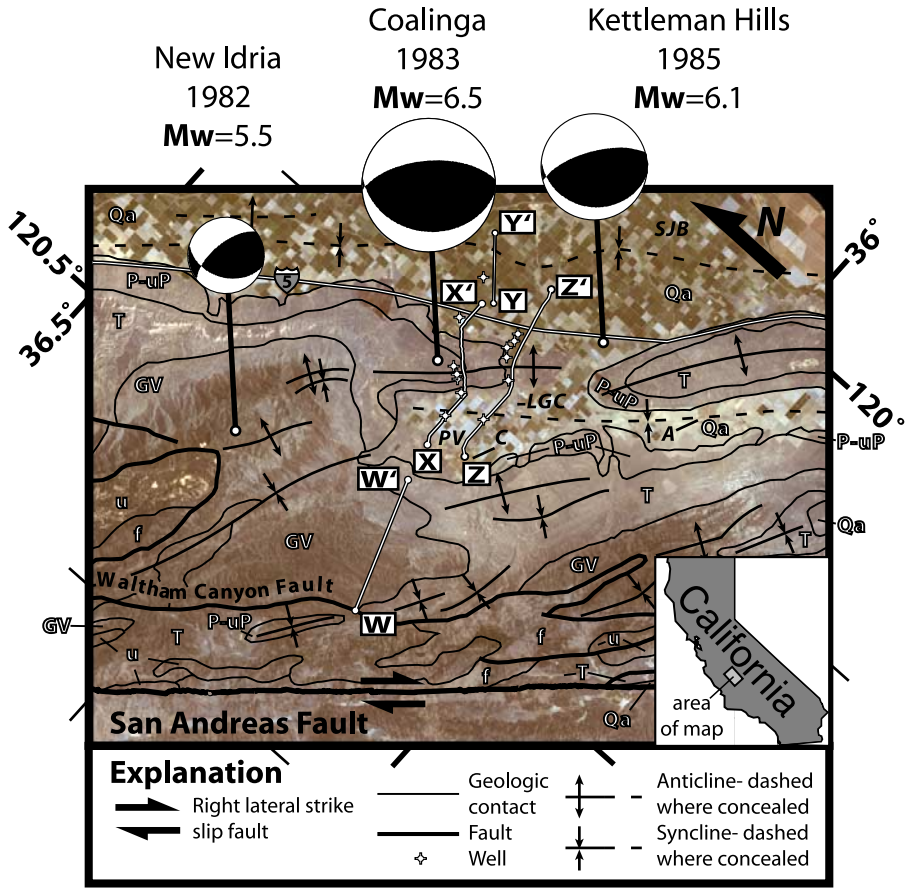

Figure 1. Landsat image and structural and generalized bedrock geology of the New Idria, Coalinga, Kettleman Hills region of the San Joaquin basin, California. The hypocentral location and focal mechanisms for the 1982 New Idria, 1983 Coalinga, and 1985 Kettleman Hills earthquakes are shown following *Stein and Ekström* [1992]. The locations of the three seismic lines (X-X′, Y-Y′, Z-Z′) and one geologic cross section (W-W′) following *Mansfield* [1991] that are presented in this study are shown. Geologic units following *Bartow* [1990, and references therein] include Qa, Quaternary alluvium; P-uP, Pleistocene to upper Pliocene sedimentary rocks; T, Tertiary sedimentary rocks; GV, Cretaceous to Jurassic Great Valley sequence; f, Mesozoic Franciscan assemblage; and u, Mesozoic ultramafic rocks. The locations of wells listed in Table 1 are shown. The locations of Coalinga (C), Avenal (A), Pleasant Valley (PV), the San Joaquin basin (SJ), and Los Gatos Creek (LGC) are indicated.

we describe the geometry and kinematics of the Coalinga anticline using two-dimensional (2-D) seismic reflection profiles, petroleum well data, earthquake focal mechanisms, and surface geology. Additionally, we relocate earthquakes from a 22 year period to investigate the 3-D nature of seismicity along the Coalinga anticline, in the context of our interpretation of the structural geometry. We use these data to construct a kinematically viable and retrodeformable, balanced cross section of the Coalinga anticline which provides evidence that the anticline is underlain by a stack of imbricated structural wedges that sole to a common upper detachment. This detachment acts as a back thrust forming a structural wedge. Additionally, our modeling indicates that the surface manifestation of the anticline is generated by a shallow thrust fault emanating from this roof thrust and not directly by the thrust ramp that ruptured during the 1983 main shock. Through our earthquake analysis, we find that the majority of the aftershock earthquakes following the 1983 event and the subsequent moment release occurred directly above the fault plane derived from our kinematic analysis. This pattern of moment release is compatible with the strain predicted for numerical models of wedge emplacement.

2. Geologic Setting

[5] The Coalinga anticline lies near the northern end of a 110 km long fold and thrust belt on the western edge of the San Joaquin basin [*Namson and Davis*, 1988; *Medwedeff*, 1989; *Stein and Ekström*, 1992]. This fold and thrust belt includes from south to north, the Lost Hills anticline, the Kettleman Hills South, Middle, and North Domes, Coalinga, and the New Idria anticlines. The northern most anticlines have documented historic seismicity beneath them [*Stein and Ekström*, 1992], including the southward propagating sequence of thrust related earthquakes beneath the New Idria (1982, M_w = 5.4), Coalinga (1983, M_w = 6.5), and Kettleman Hills (1985, M_w = 6.1) anticlines. These structures strike parallel to the San Andreas fault (Figure 1)

Table1. Wells Used in Cross Sections X-X′, Y-Y′, and Z-Z′[a]

Well	Operator	Name	Total Depth, feet	S/T/R
		Cross Sections X-X′ and Y-Y′		
1	Richard S. Rheem	Rheem Standard 28	7,753	15/20S/15E
2	Richard S. Rheem	Zwang 1	7,925	14/20S/15E
3	Gulf Oil Corp. of Calif	Leavitt-Hintze 1	8,102	12/20S/15E
4	Tidewater Oil Co.	Guardian 66	7,200	12/20S/15E
5	Holly Development Co.	82-12C	6,686	12/20S/15E
6	Reserve Oil and Gas Co.	Reserve-Union 44-33	10,443	33/19S/16E
7	Tidewater Oil Co.	Honolulu-Texas-Southern California-Southern California Petroleum Laboratories 48	13,394	25/19S/16E
		Cross Section Z-Z′		
8	The Sun Drilling Co.	P.V.F. 58-26	9,472	26/20S/15E
9	Lloyd A. Harnish	Guijarral Service 44-29P	9,199	29/20S/16E
10	Randall Oil Corp.	Guijarral Service 87X-21	9,478	21/20S/16E
11	M. I. Lebow	88-16F	8,258	16/20S/16E
12	Standard Oil Co. of Calif	Guijarral Service 51-22F	10,421	22/20S/16E
13	Union Oil Co. of Calif.	Sumpf Pleasant Valley 8-14	9,578	14/20S/16E

[a]Well locations and data from Chevron and *California Division of Oil and Gas* [1982]. S/T/R is section/township/range.

and grow due to shortening on nonemergent (blind) thrust faults that accommodate plate boundary normal compression across the San Andreas fault [*Mount and Suppe*, 1987; *Zoback et al.*, 1988]. The major phase of anticlinal growth commenced in the Tertiary based on observations of syntectonic (growth) stratigraphy that have been deposited on the limbs of the anticlines [*Namson and Davis*, 1988; *Medwedeff*, 1989; *Wentworth and Zoback*, 1990; *Bloch et al.*, 1993], although previous episodes of deformation are also documented [*Meltzer*, 1989; *Bloch et al.*, 1993]. The long-term slip rates of these faults as determined by the growth stratigraphy are in the range of 3 to 0.5 mm/yr [*Medwedeff*, 1989; *Ekström et al.*, 1992; *Stein and Ekström*, 1992; *Bloch et al.*, 1993], which is consistent with the modern day rates of fault-normal compression on the San Andreas as measured by space-based geodesy (GPS) [*Argus and Gordon*, 2001].

[6] The seismotectonics of the Coalinga anticline have been explored in previous works, inspired in large part by the 1983 earthquake, which occurred at a depth of 9.65 km beneath the crest of the fold (Figure 1). There is historic evidence that several such moderate events (**M** = 5–6.2) have occurred in this region in the past 100 years, as discussed by *Stein and Ekström* [1992]. Past studies have interpreted the 1983 earthquake as occurring on a thrust fault within a complex system of fault splays that extend from seismogenic depths upward into the core of the anticline [*Meltzer*, 1989; *Namson and Davis*, 1988; *Wentworth and Zoback*, 1990]. The complexity of deformation in the anticline is evident in the variety of aftershock focal mechanisms that were observed following the main shock event [*Eaton*, 1990; *Eberhart-Phillips and Reasenberg*, 1990; *Stein and Ekström*, 1992]. Indeed, ambiguity in determining the true rupture plane from the two nodal planes of the focal mechanism was compounded by spatially diffuse aftershocks, which occurred along both the shallow southwest dipping and steep northeast dipping nodal planes [*Eaton*, 1990; *Eberhart-Phillips and Reasenberg*, 1990; *Stein and Ekström*, 1992]. Geodetic based fault rupture models showed that slip on either plane is equally permissible [*Wentworth and Zoback*, 1990; *Stein and Ekström*, 1992], but when coupled with the spatial and temporal distribution of aftershocks immediately following the main shock [*Eberhart-Phillips and Reasenberg*, 1990], the seismologic data overall tend to favor the shallow southwest dipping nodal plane as being the main rupture plane. Following this seismologic based interpretation, fault slip models based on geodetic observations of uplift across the surface expression of the anticline tend to predict southwest dipping listric or kinked ramp fault geometries with the tip of the fault dying in the core of the anticline [*Wentworth and Zoback*, 1990; *Stein and Ekström*, 1992].

3. Structural Interpretation

[7] In this section, we use 2-D seismic reflection profiles and well data (listed in Table 1) across the Coalinga anticline that were not available in previous studies, to model the subsurface geometry of the structure, investigating the shape of both the fault ramp that ruptured during the 1983 event, as well as quantifying the slip history of the other faults underlying the anticline.

[8] Transect X-Y′, composed of seismic lines X-X′ and Y-Y′ shown in Figure 2, is a migrated and depth converted seismic reflection profile that strikes 40° across the anticline (Figure 1), within 3.7 km of the Coalinga main shock. Depth conversion of these seismic reflection profiles was conducted using the regional 3-D velocity model of *Eberhart-Phillips* [1989] so as to be more directly compatible with the velocity field used to locate published focal mechanism solutions [*Stein and Ekström*, 1992], which were incorporated into our structural interpretation. Although a few kilometers to the north, this line as a whole images structure similar in style to the seismic reflection profiles studied by *Meltzer* [1989] and *Wentworth and Zoback* [1989, 1990]. From this seismic line we can make several observations that are essential to our structural interpretation. Beneath the surface expression of the anticline, the structure in the seismic image has a narrow west dipping forelimb and a long, gently east dipping back limb. This fold shape is compatible with a westward sense of vergence related to motion on an underlying, east dipping

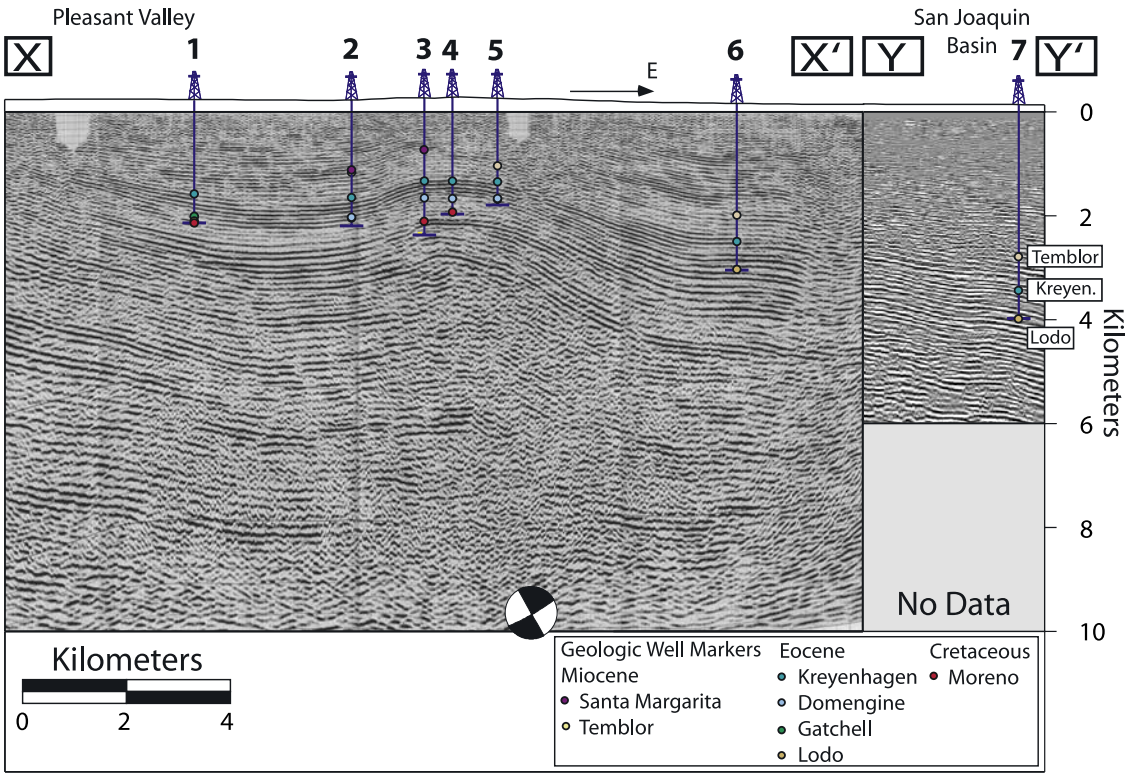

Figure 2. Uninterpreted, migrated, and depth-converted seismic profile with several wells showing formation tops across the Coalinga anticline. Note the structural relief between Pleasant Valley to the west (left) side and the San Joaquin Valley to the east (right) side. The well numbers follow those listed in Table 1, where the well locations are shown in Figure 1. The projected focal mechanism (compressional quadrant shaded) from the 1983 Coalinga (M_w = 6.5) earthquake is shown [*Eberhart-Phillips*, 1989; *Stein and Ekström*, 1992].

thrust fault. However, this asymmetric anticline is superimposed on a broader structure that is indicated by structural relief across the Coalinga anticline, where the region near Pleasant Valley is uplifted relative to the San Joaquin valley. This pattern of structural relief requires a southwest dipping thrust ramp, where slip on the fault ramp uplifts the hinterland relative to the foreland. Furthermore, to the east of the Coalinga anticline, there is a second tier of structural relief, between the Coalinga anticline and the interior of the San Joaquin Valley. This fold limb is best shown in the migrated seismic line Y-Y′ in Figure 2, where strata at a shallow depth dip down into the basin. As observed by *Wentworth and Zoback* [1990], these two tiers of broad structural relief require at least two separate ramps that have an eastward sense of thrusting, compatible with the 1983 main shock.

[9] Using these observations, we present a new structural interpretation of the Coalinga anticline as an imbricate structural wedge (Figure 3). In this interpretation, several imbricated faults generate the main fold. Slip on two separate west dipping thrust ramps, which we call the Coalinga and San Joaquin ramps, generates two anticlinal fault bend folds [*Suppe*, 1983] and the observed structural relief. Fault bend folding has been used to model other segments of the fold belt (e.g., Lost Hills, by *Medwedeff* [1989]), and these solutions imply that several kilometers of slip extends east beyond the Coalinga anticline. Seismic data east of Coalinga image undeformed strata and thus show no local evidence of a fault or detachment extending basinward of the Coalinga anticline. Thus we invoke a system of structural wedges [*Medwedeff*, 1992] to model the first-order geometry of the Coalinga anticline, where the two fore-thrust ramps share a common upper detachment surface and merge with back thrusts to generate the gross morphology of the Coalinga anticline.This wedge interpretation is consistent with the imaged fold being produced by a hybrid of classic and shear fault bend folding [*Suppe*, 1983; *Suppe et al.*, 2005]. In this model, slip on the upper fault ramp causes folding of the Coalinga anticline, whereas displacement of the lower thrust ramp focuses deformation in a buried monoclinal limb that lies to the east of the mapped anticline. On the basis of focal mechanism locations, the 1983 Coalinga (M_w = 6.5) main shock ruptured the lowermost of these two ramps (Figure 3).

[10] Evidence for older deformation can be seen in the Coalinga structure, where the structural wedge associated with the Coalinga ramp refolds and "captures" two older and shallower folds. Axial surfaces define the forelimb of one of these captured structures and growth strata within this fold limb indicate that slip on its causative fault began in the upper Cretaceous and ended in the Eocene (between the deposition of the Great Valley sequence and having ended prior to the deposition of the Domengine sandstone). On the basis of sequential models of the growth of the

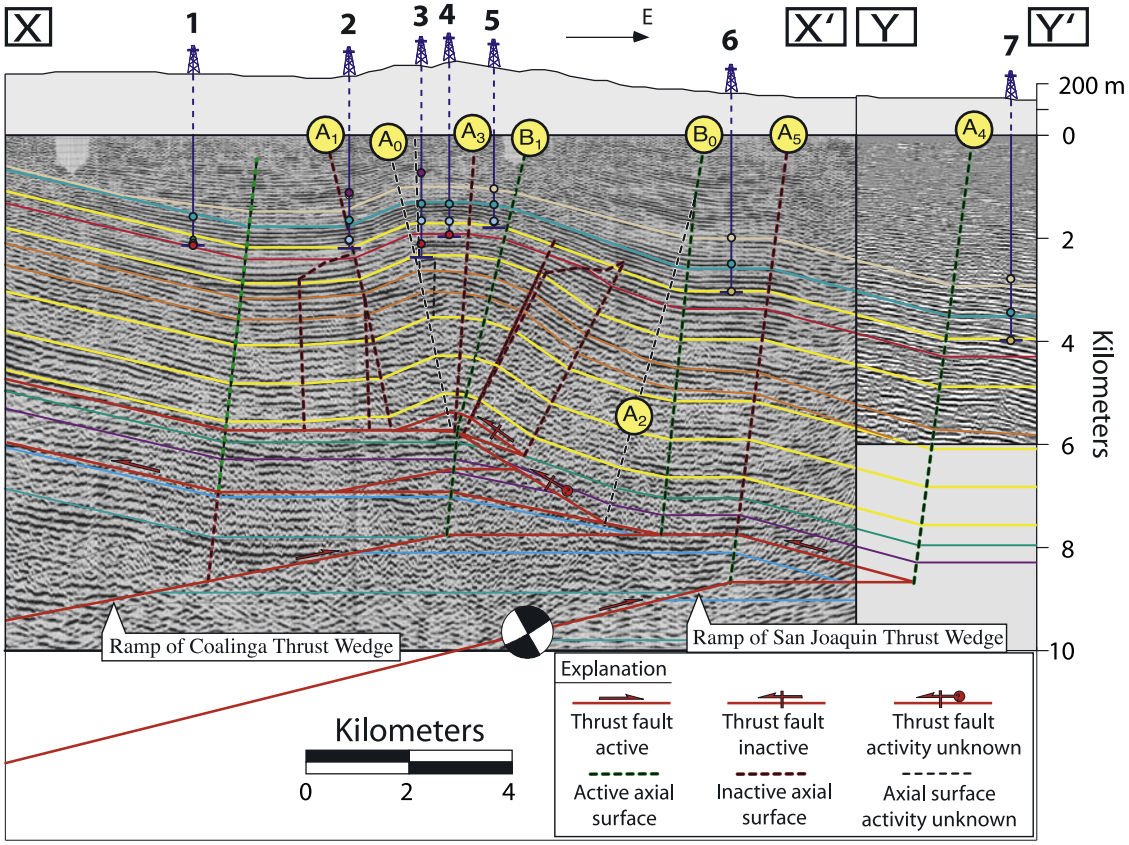

Figure 3. Geologic cross section of the Coalinga anticline. Slip on the two separate deep ramps, the Coalinga and San Joaquin ramps, generates two anticlinal fault bend folds and the two observed tiers of structural relief, defined by the kink bands between axial surfaces B_0 to B_1 and A_4 to A_5. Constrained by a pair of axial surfaces (B_0 to B_1), the forelimb of the Coalinga structural wedge refolds both an earlier structural wedge and a shallower thrust fault. This shallow thrust fault branches off of the main detachment and generates the prominent fault-related fold of the Coalinga anticline proper (constrained by axial surfaces A_0 to A_1). Slip on the San Joaquin ramp creates this fault-related fold as well as the basin-bounding structural wedge (constrained by axial surfaces A_4 to A_5). Formation depths are from wells listed in Table 1. The projected focal mechanism (compressional quadrant shaded) from the 1983 Coalinga (M_w = 6.5) earthquake is shown [*Eberhart-Phillips*, 1989; *Stein and Ekström*, 1992]. Axial surface activity refers to fold axes where modern sediments would (active) and would not (inactive) be actively folded with progressive deformation. The topography is shown at 5X vertical exaggeration.

Coalinga anticline [*Guzofski and Shaw*, 2005], the termination of this syntectonic growth strata indicate that this fold limb was created before the development of the broad limb associated with the Coalinga structural wedge that refolds it.

[11] The prominent forelimb of the Coalinga anticline that is expressed at the surface records slip on a fault that has branched off of the modeled upper detachment surface. In this interpretation, the surface expression of the Coalinga anticline is a west vergent fault bend fold related to this thrust, which splays off of the main back thrust. However, the asymmetric shape of the Coalinga anticline, with the short forelimb and the broad back limb is incompatible with a simple fault bend fold anticline solution [*Suppe*, 1983]. Therefore we interpret that there is a minimal amount of hanging wall simple shear [*Suppe et al.*, 2005] occurring above the main roof thrust, leading to a gentle back limb and a more steeply dipping forelimb with constant slip (Figure 3). As this fault is not necessarily linked directly to the fault ramp that ruptured during the 1983 event, its current activity is uncertain. Indeed, *Atwater et al.* [1990] found that the alluvial plains exposed in Los Gatos Creek across the nose of the anticline have undergone little to no folding in the Late Holocene, indicating that anticlinal growth occurs at less than 1 mm/yr, with the possibility that the structure is currently inactive. Further seismologic evidence for its activity will be discussed in section 5.3.

[12] These same main structural elements are observed in the subsurface further to the south, near the plunging nose of the Coalinga anticline. Line Z-Z′, which is shown in Figure 4, crosses the Coalinga anticline near the southern terminus of its surface expression. This line documents the continuity of the main structural elements, which include the prominent forelimb (defined by axial surfaces A_0–A_1) previously mentioned and several kilometers of structural relief between Pleasant Valley and the San Joaquin basin. Absent in this line, however, is evidence for the two tiers of structural relief present in Figure 3, suggesting that slip on one of the faults dies out to the south beneath the Coalinga

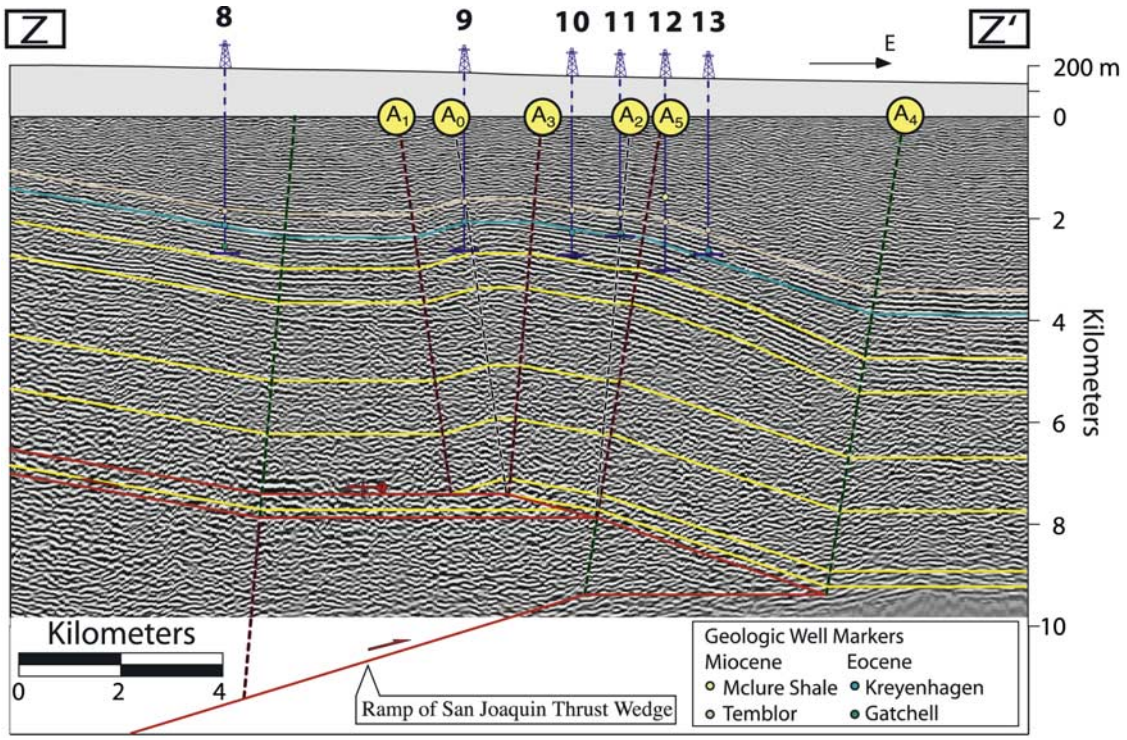

Figure 4. Geologic cross section of a migrated and depth-converted seismic reflection profile through the nose of the Coalinga anticline, identifying similar structural elements as in Figure 3. Here, the structural wedge associated with the San Joaquin ramp generates the basin-bounding monocline (constrained by axial surfaces A_4 to A_5), as a smaller displacement thrust branches off to generate the prominent forelimb of the anticline (constrained by axial surfaces A_0 to A_1). The lack of further structural relief across the center of the anticline suggests that the Coalinga ramp and associated wedge structure is not present at this location along the anticline. The topography is shown at 5X vertical exaggeration. Formation depths are from wells listed in Table 1, and the remaining symbols follow Figure 3.

anticline. This is compatible with the overall plunge and diminished surface expression of the Coalinga anticline to the south. Continuity along strike of the syncline that pins the location of the eastern most wedge tip suggests that the San Joaquin ramp continues to the south to line Z to Z′. Therefore, as slip on the Coalinga ramp dies out, the broad fold plunges and its surface expression diminishes. This implies that shortening must be accommodated on the San Joaquin ramp or another structure, such as the Jacalitos anticline [*Dibblee*, 1971], which emerges directly to the southwest of the Coalinga anticline, where slip on the Coalinga ramp dies out (Figure 1). To the north of our sections, the two tiers of the Coalinga anticline continue with increased slip and structural relief on the Coalinga wedge, as shown in the seismic reflection profile SJ-3 of *Namson et al.* [1990].

4. Regional Context of Wedge Interpretation

[13] As previously identified, the lack of basinward deformation requires that slip on the deep fault ramps is either consumed by a fault propagation folding mechanism [*Suppe and Medwedeff*, 1990; *Erslev*, 1991] or is sent back to the hinterland on a back thrust, forming a structural wedge [*Medwedeff*, 1992]. Each has a different associated geodynamic and seismic hazard implication, most notably the structural wedge model requires a shallow back thrust to extend to the west beneath the anticline. Both types of structures have been interpreted elsewhere on the western edge of the San Joaquin basin [*Namson and Davis*, 1988; *Namson et al.*, 1990; *Medwedeff*, 1989; *Bloch et al.*, 1993]. However, in general, kinematic models of fault propagation folding predict steeply dipping beds at or near the fault tip as slip is consumed [*Suppe and Medwedeff*, 1990; *Allmendinger*, 1998], which we do not see at the leading edge of the Coalinga and San Joaquin fault ramps. Rather, we observe fold limbs with consistently low-angle dips, compatible with a fault bend folding and structural wedging solution [*Suppe*, 1983; *Medwedeff*, 1992].

[14] The structural wedge interpretation implies that we should observe southwest vergent structures and/or eastward dipping thrust faults exposed at the surface in the hinterland. *Dickinson* [2002] presented evidence against previous models of the Coalinga anticline as a structural wedge, that invoked Franciscan metasediments being thrusted above the main fault ramp in the core of the fold [*Wentworth and Zoback*, 1990]. In this work, *Dickinson* [2002] demonstrated that the petrophysical properties of the rocks modeled to be the Franciscan wedge beneath Coalinga are similar to the Upper Jurassic to Cretaceous Great Valley group exposed in the foothills of the anticline. More importantly, it was observed that the Great Valley group rocks exposed in the hinterland project down beneath the Coalinga anticline, into the region of the fold that had

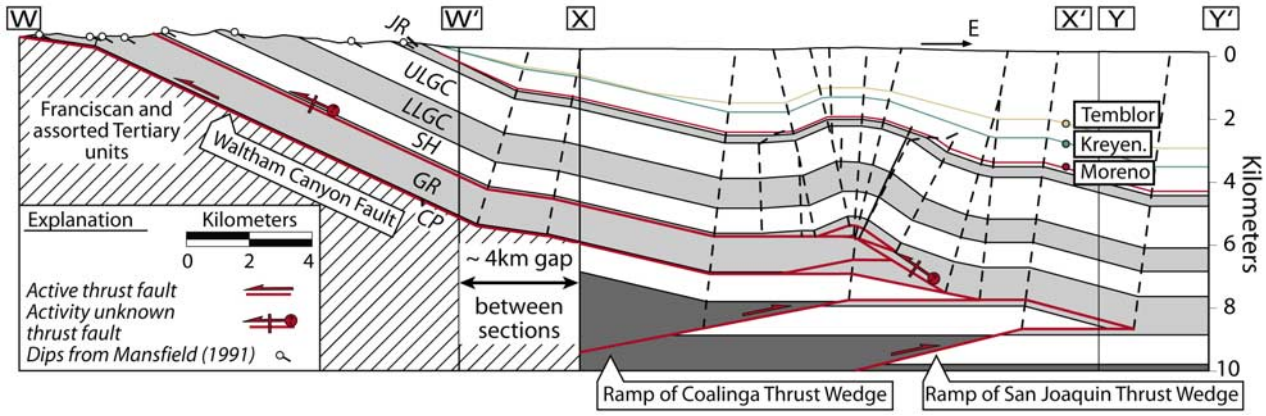

Figure 5. Structural interpretation through Coalinga anticline extended to intersect the foothills near the cross section W-W′ after *Mansfield* [1991]. The mapped petrofacies units of the Cretaceous Great Valley group exposed in the foothills extends beneath the Coalinga anticline, with the back thrust/roof thrust of the structural wedge intersecting the surface as the Waltham Canyon fault. For this interpretation to be plausible, up to ~7 km of slip must be taken up on the Waltham Canyon fault, as prescribed by the kinematic model. Tertiary units interpreted in X-Y′ were extrapolated to line W-W′ based on regional work by *Bartow* [1990] and surface exposures. The Great Valley units are JR, Joaquin Ridge; ULGC, Upper Los Gatos Creek, LLGC, Lower Los Gatos Creek; SH, Studhorse; GR, Grabast; CP, Center Peak. Dashed lines are axial surfaces. The interpretation in the gap between W′ and X is based on seismic data to the south extrapolated along strike.

previously been interpreted as the Franciscan wedge. From this analysis and based on the projection of the back thrusts interpreted by *Wentworth and Zoback* [1989, 1990] into unfaulted rocks in the hinterland, *Dickinson* [2002] supported this view that the Coalinga fold did not form as a structural wedge.

[15] To reevaluate the surface exposure of the back thrust of the structural wedge, we extend our structural interpretation further to the west into the hinterland near the previously published cross section of *Mansfield* [1991] as shown in Figure 5 following *Dickinson* [2002]. The main candidate for the outcropping back thrust of the structural wedge is the Waltham Canyon fault [*Dibblee*, 1971; *Namson and Davis*, 1988; *Wentworth and Zoback*, 1990; *Mansfield*, 1991], which thrusts Jurassic-Cretaceous (Great Valley) to Tertiary rocks onto Jurassic (Franciscan) to Tertiary rocks. As shown in Figure 5, the Waltham Canyon fault does appear to link directly to the back thrust related to the Coalinga and San Joaquin ramps defined in our analysis. This is due to the fact that we model the San Joaquin ramp, which ruptured in the 1983 event, as stepping up to a basal detachment to define the wedge tip at a greater depth than has been previously interpreted. It should be noted that the main constraints on the depth of the fault ramp are the fold limb geometry at the edge of San Joaquin basin and the main shock focal mechanism location [*Eberhart-Phillips*, 1989; *Stein and Ekström*, 1992], which has an estimated error in the focal depth location of 200 m [*Eaton*, 1990]. Regardless of these uncertainties, our balanced structural interpretation demonstrates that it is reasonable for the back thrust of the San Joaquin and Coalinga ramps to breach the surface as the Waltham Canyon fault. Our solution implies that there is nearly 7 km of displacement on this fault or faults subparallel to it. Unfortunately, we cannot constrain slip on this fault as a test of our structural solution because the Waltham Canyon fault locally dips subparallel to the rocks in its hanging wall and its footwall, as shown in our structural interpretation and cross section (Figure 5). However, this analysis is independent of the presence or absence of Franciscan crust within the wedge itself [*Wentworth and Zoback*, 1989, 1990; *Dickinson*, 2002], as we simply conclude that the Cretaceous Great Valley group is locally thrust upon the Franciscan within the foothills, based on map patterns of the Waltham Canyon fault [*Dibblee*, 1971].

5. Seismicity of the Coalinga Wedge

[16] The spatial association of the Coalinga anticline and the 1983 earthquake sequence, as well as geodetically observed coseismic uplift patterns argue that the anticline grows by slip on the underlying blind thrust system [*Stein and King*, 1984]. However, the complex fault geometry constrained by seismic reflection profiles and kinematic modeling in this study is strikingly different from the fault geometry that was derived by geodetic and seismologic techniques alone [*Wentworth and Zoback*, 1990; *Stein and Ekström*, 1992]. Our structural interpretation argues for a more complex mechanism of fold growth, with several faults and structural wedges contributing to the development of the anticline. Thus, in light of our new structural interpretation, we reevaluate the seismicity patterns near Coalinga following the 1983 event to investigate the relationship between blind-thrust earthquakes and fold growth. Recent seismotectonic analyses in southern California have benefited from the complementary assessment of geologically constrained structural models and improved earthquake catalogs to constrain the earthquake hazards associated with blind-thrust faults [*Shaw and Shearer*, 1999; *Carena and Suppe*, 2002]. Therefore, in section 5.1 we present a new relocated earthquake catalog which we use to investigate patterns of faulting and event moment distribu-

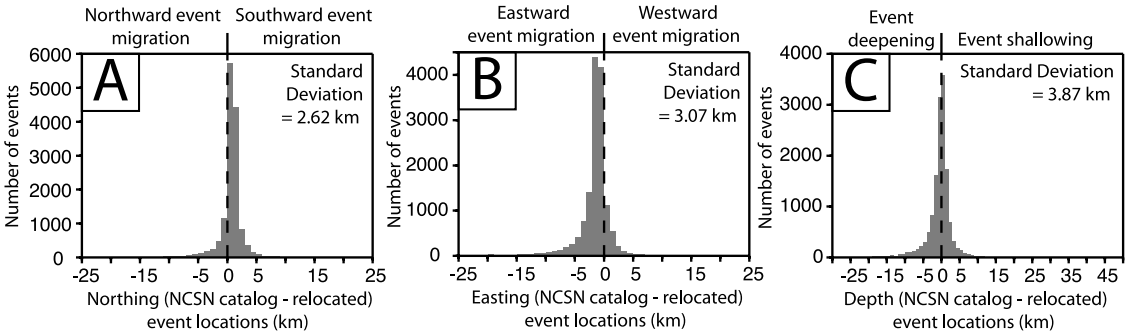

Figure 6. Histograms of the change in event locations, showing the effect of applying the relocations methods to the event catalog for the Coalinga area. (a) The change in the northing of the events, where a positive distance indicates the event moved to the south. (b) Change in the easting of the events, where a positive distance indicates the event moved to the west. (c) Change in the depth of the events, where a positive depth change indicates the event moved to shallower depths.

tion as related to coseismic deformation of the Coalinga wedge.

5.1. Relocated Earthquakes

[17] To improve the seismic event locations, we relocated 14,509 earthquakes from the Northern California Seismic Network (NCSN) spanning 1980 to 2002 in the Coalinga region with the source-specific station term (SSST) method [*Richards-Dinger and Shearer*, 2000; *Lin and Shearer*, 2005; *Shearer et al.*, 2005]. This technique uses a grid search, L1 norm approach to locate the events, iterating to generate spatially varying delay times that are specific to each source region. This greatly improves the relative location accuracy of nearby events by accounting for the biasing effects of traveltime anomalies caused by 3-D velocity structure. For these relocations, we used the 1-D NCSN velocity model for the Coalinga region and existing P and S phase pick information. However, to constrain better the absolute event locations, we computed station terms using locations (D. Eberhart-Phillips, personal communication, 2003) from a previous joint hypocenter velocity inversion for the 1178 events between 4 May 1983 and 30 June 1983 and used these station terms as the starting station terms for our SSST relocations of the complete set of events. Locations were further refined for an additional 2737 events by applying waveform cross correlation and cluster analysis as described by *Shearer et al.* [2005]. In this method, P and S wave cross-correlation functions are computed for events with similar waveforms. This allows for the calculation of differential times for each event pair, which can often be measured to subsample precision for similar events, allowing relative earthquake location precision to a few tens of meters. Histograms of the magnitude of event relocation (Figure 6) demonstrate that these techniques tended to migrate events in the region to the southeast, by several kilometers.

[18] To investigate further the event location change, Figure 7 shows a cross section of events from the original NCSN catalog and the same events relocated using the SSST method across the Coalinga anticline along section X-X′. Overall, as has been seen for similar relocated catalogs of blind-thrust events [i.e., *Shearer*, 1997], the events tend to cluster together in discrete regions, adding further definition to previously observed bands of seismicity [*Eaton*, 1990; *Eberhart-Phillips and Reasenberg*, 1990]. The largest cluster of events from both catalogs dips down to the left (southwest), compatible with the preferred nodal plane of the 1983 main shock and the San Joaquin ramp. However, the events cluster more tightly in this fault rupture zone in the relocated catalog. Yet, as shown in these comparisons, even in the relocated catalog there are still a significant number of events that are not associated with the main shock rupture plane or other discrete faults but are distributed at shallow depths. This result demonstrates that the observed pattern of these secondary earthquakes in the hanging wall is truly a product of deformation related to blind thrust fault-related folding. These events likely demonstrate bedding parallel slip and secondary faulting in response to folding, as will be further discussed below.

5.2. Structural Compartmentalization of Seismicity

[19] *Eaton* [1990] and *Eberhart-Phillips and Reasenberg* [1990] investigated the complex faulting history demonstrated by aftershock focal mechanisms beneath the Coalinga anticline following the 1983 event. As mentioned above, we find that many of the first-order features that have been previously identified, such as seismicity lineations proximal to the main shock, are further highlighted by the relocation techniques. Therefore we focus our analysis on the event and moment distribution for the aftershocks in our relocated catalog as they relate to our interpreted structural model. Primarily, we are interested in how the distribution and moment magnitudes of the events vary with respect to a 3-D model of the San Joaquin fault plane where it is constrained by seismic reflection data. Additionally, our investigation is motivated by the observation of significant hanging wall deformation, with earthquakes that have a range of modes and intensities. We seek to test whether there is a relationship between seismicity and structural compartments as defined by fold kink bands and secondary faults.

[20] As the NCSN catalog events used in this study span several decades and magnitude scales, there is significant variation in the type of magnitudes that are reported for each event. In order to investigate spatially varying seismic energy release, we converted the reported earthquake mag-

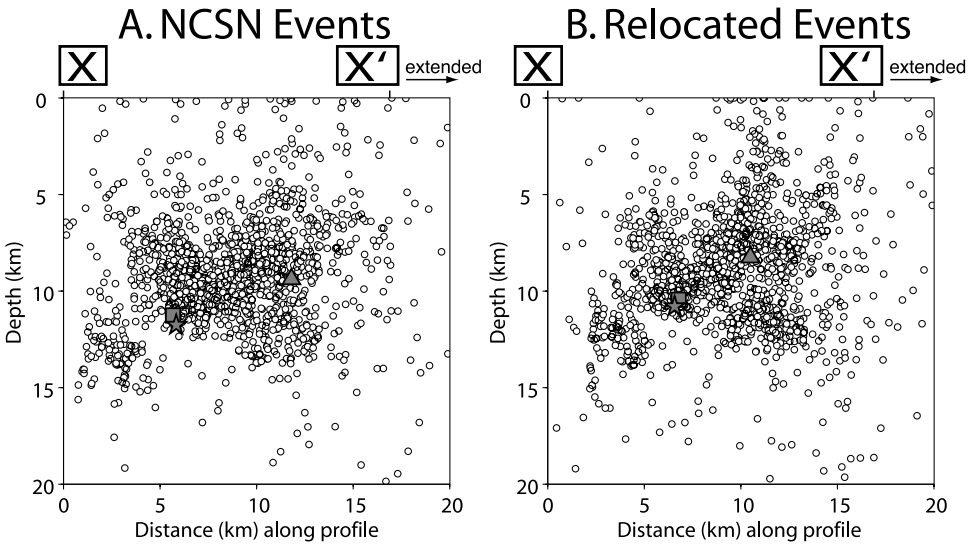

Figure 7. Cross section along line X-X′ showing the events (circles) within 3 km of the section (extended ~4 km along strike to include structure from Y-Y′) from the (a) NCSN catalog compared to the (b) events relocated in this study, using just the station terms. For comparative purposes the three largest earthquakes that are included in both sections are shown as alternative symbols (triangle, star, and square). These three events tended to migrate together to be within the west dipping cluster.

nitudes to seismic moment using the empirical relationships of *Bakun* [1984] and *Thatcher and Hanks* [1973] as listed in Table 2. Nearly all of the events have reported magnitudes, which includes 178 events reported to have zero magnitude. In light of the fact that we are spatially summing moment, the impact of these events is minimal.

[21] The combination of our spatially registered structural interpretations and seismic reflection profiles further to the north allow us to construct a 3-D representation of the southwest dipping San Joaquin fault ramp (see Figure 8a). While the ramp likely continues further north toward the New Idria anticline, the distribution of our seismic reflection data does not allow us to constrain it there. Regardless, we are primarily interested in testing the relationship between our structural model and seismicity patterns near the 1983 main shock. Figure 9a shows the moment distribution of relocated events normal to our 3-D fault surface, while Figure 9b shows the overall event distribution. It is not surprising that the largest moment release of the events occurs proximal to the fault surface, as it was constructed using available focal mechanism solutions [*Eaton*, 1990; *Stein and Ekström*, 1992], including the main shock, and fault-related folding techniques. However, the skewed event distribution, with more events occurring in the hanging wall, is not a result that we would expect to be prescribed by our fault plane solution (Figure 9b). The maximum distribution of events is centered directly above zero or, in another sense, directly above the fault plane, but there is a discrete drop in the density of events directly beneath the fault plane. In the San Joaquin basin and nearby, it is believed that temperature-dependent aseismic processes should not begin to be the dominant deformation mechanism until depths of 14 to 15 km [*Namson et al.*, 1990; *Murray et al.*, 2001]. Therefore the increased dominance of aseismic creep with depth cannot be the sole mechanism to explain this sharp step in aftershock distribution proximal to the thrust ramp along its entire extent. Furthermore, models of stress changes following the 1983 main shock do not predict asymmetric patterns of stress distributions [*Stein and Ekström*, 1992; *Lin and Stein*, 2004], arguing that for uniform hanging wall and footwall materials, the pattern of aftershocks responding to these stress perturbations should be roughly symmetric, as observed in other blind-thrust events [*Shearer*, 1997; *Shaw and Shearer*, 1999; *Carena and Suppe*, 2002].

[22] To explore further this asymmetry in event distribution, we looked at the moment density distribution from the earthquakes as they relate to broad structural compartments in our kinematic model. This was accomplished by dividing our structural model into three regions; region 1 the sedimentary cover above the uppermost back thrust, region 2 the structural wedge, and region 3 corresponds to the footwall of the San Joaquin ramp as shown in Figure 10. We then summed the moment of the earthquakes that occurred in each of the structural regions and calculated the moment density for that region for comparison. The results of this calculation are given in Table 3, which shows that in addition to there being more events within the wedge

Table 2. Empirical Relations Used to Convert NCSN Catalog Magnitudes to Seismic Moment[a]

NCSN Catalog Magnitudes	Conversion Equation	Reference
M_d	$\log(M_o) = 1.2M_d + 17$	*Bakun* [1984]
M_x, M_L, M_lg	$\log(M_o) = 1.5M_{x,L,lg} + 16.0$	*Thatcher and Hanks* [1973]
M_w	$M_w = \frac{2}{3}\log(M_o) - 10.73\}$	

[a]In units of dyn cm.

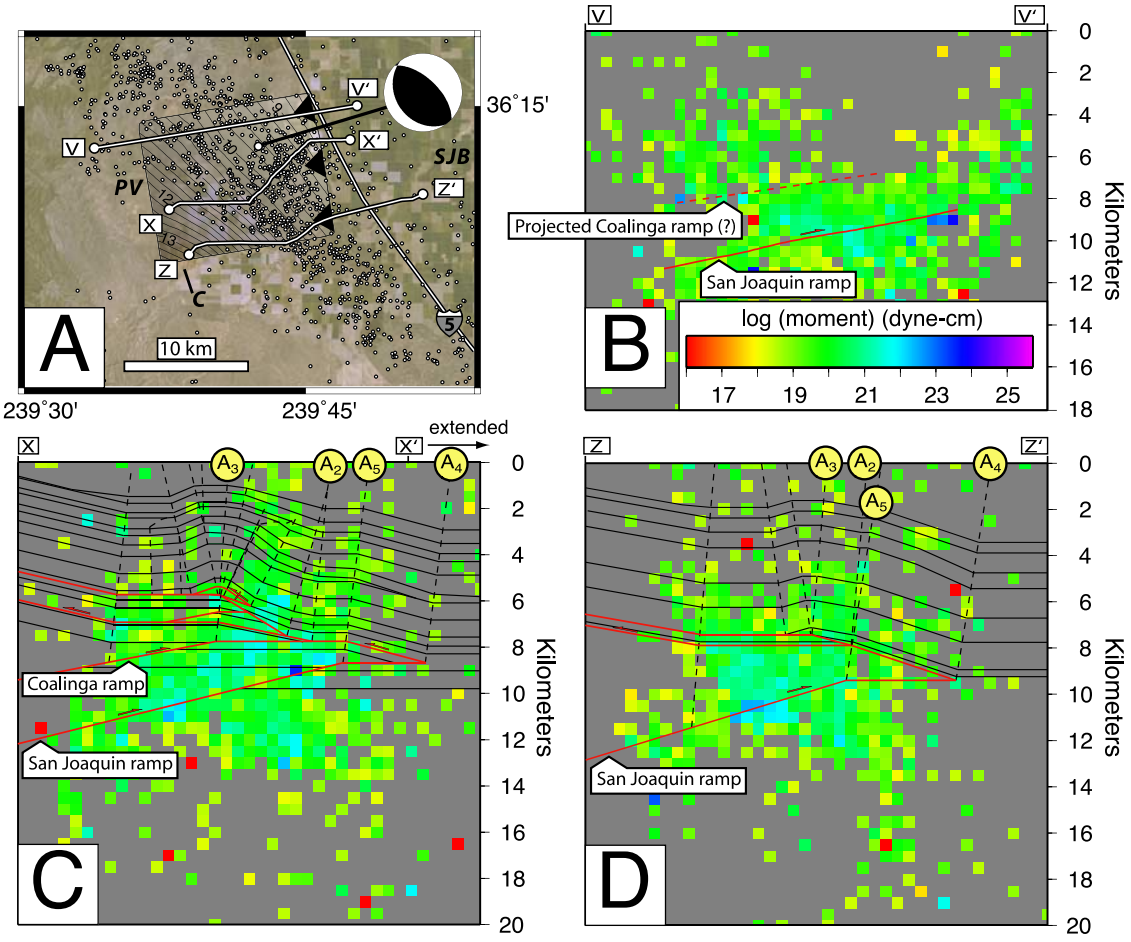

Figure 8. Distribution of summed moment compared to regional cross sections. In all lines the moment was summed in cells 500 × 500 m, with events from 3 km away projected into the plane of the section. (a) Location map of the Coalinga anticline, showing the extent of the San Joaquin ramp (shaded surface with 200 m contour intervals, labeled at every km) related to lines X-X′, Z-Z′, and V-V′. The white circles show events from our relocated catalog that have seismic moments greater than 10^{20} dyn cm. The remaining symbols follow Figure 1. The focal mechanism from the 1983 Coalinga (M_w = 6.5) earthquake is shown [*Eberhart-Phillips*, 1989; *Stein and Ekström*, 1992]. (b) Line V-V′ showing the summed moment distribution near the end of the mapped San Joaquin ramp. Projected on the section is the possible location of the Coalinga ramp following line X-X′. (c) Line X-X′ (extended ~4 km along strike to include structure from Y-Y') showing the summed moment distribution relative to the structural interpretation. As discussed in the text, moment release in the hanging wall of the wedge appears to be mainly limited to the fold limb above the branching back thrust (constrained by axial surfaces A_2 to A_3). (d) Line Z-Z′ showing the summed moment distribution relative to the structural interpretation. Similar relationships between moment distribution in the hanging wall and the limb above the branching back thrust (constrained by axial surfaces A_2 to A_3) are observed. Additionally, all sections demonstrate the increased moment release within the structural wedge.

itself (i.e., region 2), it has a higher moment density than both the footwall and the sedimentary cover.

[23] The asymmetry in the event and moment distribution is most easily explained by a contrast in strain fields or material strength across the San Joaquin ramp. Numerical models of structural wedge emplacement by *Erickson* [1995] predict higher plastic strains within the wedge, compared to the footwall block. In all of the model cases presented by *Erickson* [1995], the highest strains did not necessarily occur directly at the wedge tip, but were found in the overlying cover, above the wedge tip and the back thrust, as well as within the wedge itself, directly above the fault ramp. Some of this strain in the modeled wedge is likely due to folding caused by a change in ramp geometry at depth (i.e., the modeled thrust fault ramps up from a lower detachment to a higher detachment [*Erickson*, 1995]). Yet, model elements that have been translated along the fault ramp, but not folded as is analogous to the Coalinga wedge, are also more highly strained in some model cases. These model results are compatible with the observed seismicity patterns of wedge emplacement in the Coalinga structure, as the wedge interior deforms more seismically than the footwall or the sedimentary cover directly above the ramp. This observation is highlighted by the seismicity

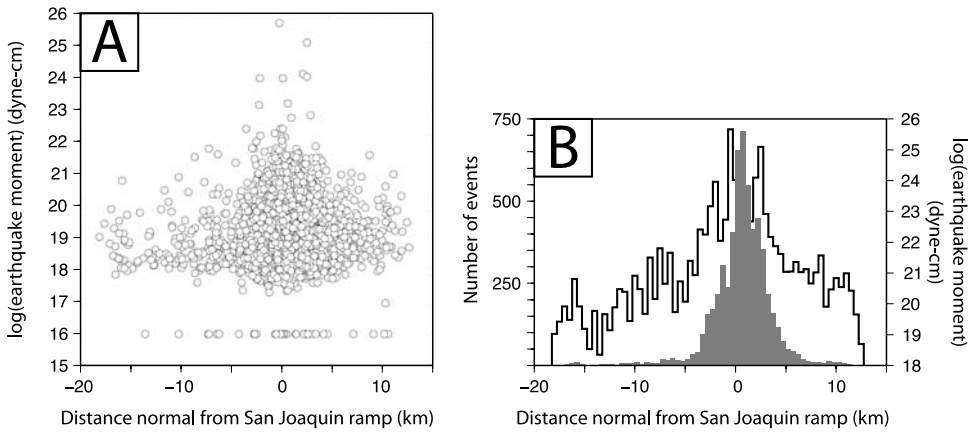

Figure 9. Relocated earthquake distribution relative to the San Joaquin ramp. (a) Plot of the moment of the earthquakes versus distance from the fault ramp. Notice that the events with the largest moment release cluster near the fault surface. Not including the 1983 main shock, the cumulative moment release of these events is $10^{25.2}$ dyn cm or ~36% of the main shock moment. (b) Histogram of event density normal to the fault ramp shown in gray and the summed moment of the earthquakes at that distance is shown by the black line. Note the steep decline in event density below (negative distance values) the fault ramp.

patterns shown in Figure 10; a significant percentage of the earthquakes with the largest moment release are on or bounded by the fault ramps and back thrusts.

[24] The distribution of seismicity and seismic moment could also be explained in part by asymmetric elastic properties across the fault ramp, as has been postulated to influence directly aftershock asymmetry on the San Andreas fault [*Rubin and Gillard*, 2000]. Numerical models of strike slip faults with laterally inhomogeneous elastic properties demonstrate that this condition leads to an asymmetric strain field proximal to the fault [*Mahrer and Nur*, 1979; *Rybicki*, 1978]. Evidence for elastic inhomogeneity across the San Joaquin ramp is provided by seismic velocity analysis in the Coalinga region. Using previously published reflection and refraction surveys that have been acquired across the Coalinga anticline [*Fielding et al.*, 1984; *Wentworth and Zoback*, 1990; *Walter*, 1990], *Popovich and Miller* [2002] developed a 3-D velocity model for the Coalinga region. This work highlighted the fact that the 1983 Coalinga main shock occurred on a velocity interface between higher velocity rocks in the footwall and lower velocity rocks in the hanging wall. This led *Popovich and Miller* [2002] to conclude that the earthquake occurred along a lithologic boundary, likely a boundary between the Franciscan basement and Great Valley sedimentary sequence in the hanging wall, based upon the modeled seismic velocities. Irrespective of the absolute lithologic distinction, if a contrast exists between the elastic strength of the materials across the fault ramp as determined from regional velocity models, this could cause an asymmetry in the seismic strain pattern as has been documented for strike-slip fault systems. Moreover, if a preexisting lithologic and strength contrast existed, it likely helped to localize the thrust ramps and detachments that formed the structural wedge. Thus both strength contrast and the structural wedging mechanism likely conspire to produce the observed patterns of seismicity and moment release in the 1983 earthquake sequence.

5.3. Seismicity and Coseismic Folding

[25] Aftershocks concentrated above the San Joaquin ramp presumably contribute to folding of the Coalinga anticline. However, the 1983 event lacked evidence of discrete, near-surface, coseismic folding, as has been observed in other blind-thrust and surface breaching reverse fault systems [*Suppe et al.*, 2000; *Dolan et al.*, 2003]. Instead, leveling surveys provided evidence that the crest of the anticline underwent several centimeters of broad uplift following the earthquake [*Wentworth and Zoback*, 1990; *Stein and Ekström*, 1992]. Seismicity patterns beneath the Coalinga anticline as shown in Figure 10 demonstrate that clusters of earthquakes in region 1, above the roof thrusts, appear to be spatially associated with fold limbs, most notably the back limb of the Coalinga anticline (see Figure 3). Thus we investigate the possibility that secondary slip on bedding parallel surfaces and faults contained within the folds limbs may contribute to the broad coseismic uplift of the Coalinga anticline through further comparisons between our structural models and the earthquake distributions.

[26] To document the moment release in the fold limbs due to aftershocks, we investigated the moment distribution of aftershocks along 3 profiles across the anticline as shown in Figure 8. Along each profile, we summed moment in bins that were 500 × 500 m along the axes of the respective section and then compared them to the structural interpretations. Figure 8b demonstrates that these first-order observations, of increased moment release in the hanging wall, continue to the northern section of the Coalinga structure. Figures 8c and 8d show the summed moment release relative to the structural interpretations in lines X-X′ and Z-Z′. In both sections, moment release in the hanging wall is localized in the back limb of the branching back thrust constrained by axial surfaces A_2-A_3. Additionally, in Figure 8d, moment release in the forelimb of the wedge associated with the San Joaquin ramp (constrained by axial surfaces A_4-A_5) is limited to axial surface A_4 that is pinned

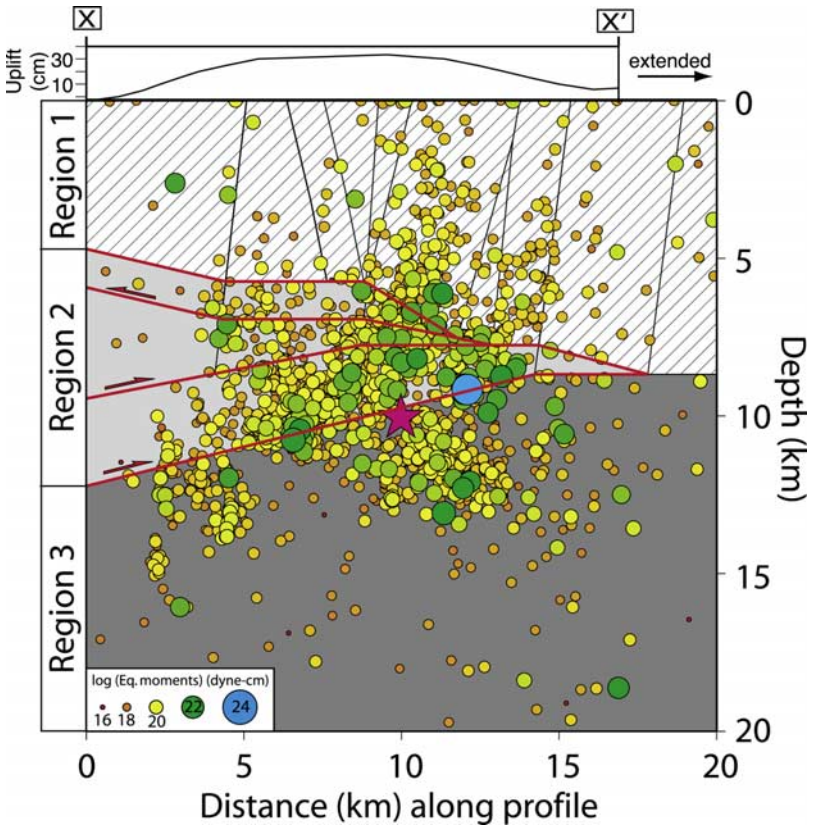

Figure 10. Earthquakes and structural regions used for moment summing compared to the structural interpretation along line X-X′ (extended ~4 km along strike to include structure from Y to Y′) and the coseismic surface uplift pattern from the 1983 Coalinga earthquake [*Stein and Ekström*, 1992]. The structural model is divided into three regions for the purpose of moment summing as shown in Table 3, where region 1 lies above the upper most roof thrust, region 2 is the structural wedge, and region 3 is the footwall of the fault ramps. The events are scaled by size and color for moment (dyn cm). The star shows the projected location of the 1983 hypocenter. Dashed lines are axial surfaces and the red lines indicate faults after Figure 3. Note that earthquakes occur throughout the region of interest, over a wide depth extent. However, the magnitude and density of events rapidly drop off with distance from the 1983 earthquake as shown in Figure 9, so our moment summing calculation is not significantly affected by the extent of the lateral boundaries of the structural regions.

to the wedge tip, suggesting that the deformation is mainly constrained within the folded structural compartment corresponding to the wedge forelimb. However, this type of relationship, within this forelimb, is not clearly observed in the section shown in Figure 8c, arguing that there is lateral variability in the seismically observable folding strains.

[27] Based upon the distribution of moment release along line X-X′ and Z-Z′ in Figures 8c and 8d, there is an increase in hanging wall moment release, roughly between axial surfaces A_2-A_3. This deformation could be related to either folding due to slip on the upper, branching back thrust and/or slip on the Coalinga ramp and wedge. While we cannot exclude the possibility that the Coalinga thrust slipped following the 1983 earthquake, we favor an interpretation that the deformation between axial surfaces A_2-A_3 is related to deformation due to slip on the shallow back thrust. This conclusion is primarily based upon the fact that we observe similar seismicity distribution patterns to the south in Figure 8d, where we have no evidence for the Coalinga wedge and ramp. In this scenario, the seismic strain in the fold limb is released by slip on bedding plane slip surfaces and/or faults that were generated as the rocks were incorporated into the fold limb between axial surfaces A_2-A_3.

[28] Secondary slip on the back-thrust and subsequent folding of the back limb might have contributed to the observed coseismic crestal uplift that was associated with the 1983 main shock. The pattern of coseismic uplift [*Stein and Ekström*, 1992] relative to our structural solution and aftershock distribution is shown in Figure 10. This pattern

Table 3. Seismic Moment by Structural Region

Region	Number of Events	Area, cm^2	Summed Moment, dyn cm	Moment Density,[a] dyn cm/cm^2
1	307	1.3×10^{12}	2.9×10^{22}	2.2×10^{10}
2	901	6.4×10^{11}	4.4×10^{23}	7.0×10^{11}
3	630	2.0×10^{12}	1.2×10^{23}	5.8×10^{10}

[a]Here moment density is defined as the moment divided by the area of the structural region.

of geodetic uplift associated with the 1983 main shock has served as a primary constraint on the geometry and slip history of the Coalinga earthquake in previous studies [*Stein and King*, 1984; *Wentworth and Zoback*, 1990; *Stein and Ekström*, 1992]. The maximum coseismic uplift was roughly centered above the main axis of the anticline, compatible with the preferred scenario of reactivation of the shallow back thrust and coseismic folding of the eastern limb of the anticline, defined by axial surfaces A_2–A_3. While this effect is not discrete, as has been observed or inferred in other cases [*Suppe et al.*, 1997; *Mueller et al.*, 1999; *Dolan et al.*, 2003], the deformation is constrained to the fold limb, and broadly uplifts the Earth's surface coseismically. In the context of the structural model presented here, active folding of the surface should occur due to slip on the Coalinga and San Joaquin ramps, as well as the back thrust that is associated with the surface manifestation of the Coalinga anticline. As has been postulated for other blind thrust systems [*Dolan et al.*, 2003], such surface fold scarps generated by folding of young sediments and slip on the underlying thrust ramps, are likely generated during significantly larger events. It is interesting to note that there was no definitive coseismic geodetic uplift signature associated with the forelimb generated by main shock slip on the San Joaquin ramp. However, the center of maximum postseismic uplift, which shifted to the east by several kilometers relative to the locus of coseismic uplift [*Stein and Ekström*, 1992], is fairly close to the crest of the monoclinal forelimb associated with the San Joaquin ramp as modeled here. This spatially shifting pattern of surface uplift is consistent with our model of the Coalinga structure developing as an imbricated stack of structural wedges, where a significant component of the seismic moment is released in aftershocks that accommodate folding in the hanging wall of the wedge. From this we can conclude that the pattern of surface uplift in relation to our structural model and relocated aftershocks demonstrates that a series of discrete faults, associated folding, and hanging wall seismicity lead to a complex uplift pattern that cannot solely be attributed to slip on a single fault ramp.

6. Conclusions

[29] We documented the subsurface structural geology and kinematics of the Coalinga anticline in the San Joaquin basin, central California. On the basis of analysis of seismic reflection data, well data, surface geology, and earthquake seismicity we find that the Coalinga anticline is underlain by two imbricated structural wedges that merge into a common roof thrust or back thrust. We provide further evidence that this back thrust breaches the surface as the Waltham Canyon fault in the hinterland, as interpreted by previous authors. Linkage of the seismogenic thrust ramp with this back thrust forms an active wedge structure, that is consistent with the complex subsurface pattern of folding imaged in the Coalinga anticline.

[30] Using these structural models, we further investigate structural controls on the patterns of seismicity in the Coalinga region using a relocated earthquake catalog. Analysis of the moment distribution of the aftershocks following the 1983 Coalinga main shock indicates that a significant majority of the coseismic deformation occurred within the core of the structural wedge, above the ramps and beneath the back thrusts. An additional component of the aftershocks is also spatially associated with fold limbs of the back thrust that branches off of the main roof thrust, arguing for coseismic fault-related folding in this active wedge structure.

[31] **Acknowledgments.** This work is supported by the NSF grant 0230141. Data and financial support were provided by Texaco, Inc. and Chevron. Aera Energy also provided support for this research. Associate Editor Jean-Philippe Avouac, Göran Ekström, and Don Medwedeff are thanked for providing insightful reviews that helped to strengthen the paper. Several figures were drafted using GMT [*Wessel and Smith*, 1991].

References

Allmendinger, R. W. (1998), Inverse and forward numerical modeling of trishear fault-propagation folds, *Tectonics*, *17*(4), 640–656.

Argus, D. F., and R. G. Gordon (2001), Present tectonic motion across the Coast Ranges and San Andreas fault system in central California, *Geol. Soc. Am. Bull.*, *113*, 1580–1592.

Atwater, B. F., D. A. Trumm, J. C. Tinsley, R. S. Stein, A. B. Tucker, D. J. Donahue, A. J.T. Jull, and L. A. Payen (1990), Alluvial plains and earthquake recurrence at the Coalinga anticline, in *The Coalinga, California Earthquake of May 2, 198*, edited by M. Rymer and W. Ellsworth, *U. S. Geol. Surv. Prof. Pap.*, *1487*, 273–297.

Bakun, W. H. (1984), Seismic moments, local magnitudes, and coda-duration magnitudes for earthquakes in central California, *Bull. Seismol. Soc. Am.*, *74*(2), 439–458.

Bartow, J. A. (1990), A summary of the Cenozoic stratigraphy and geologic history of the Coalinga region, central California in *The Coalinga, California Earthquake of May 2, 1983*, edited by M. Rymer and W. Ellsworth, *U. S. Geol. Surv. Prof. Pap.*, *1487*, 3–12.

Bloch, R. B., R. V. Huene, P. E. Hart, and C. M. Wentworth (1993), Style and magnitude of tectonic shortening normal to the San Andreas fault across Pyramid Hills and Kettleman Hills South Dome, California, *Geol. Soc. Am. Bull.*, *105*, 464–478.

California Division of Oil and Gas (1982), *Oil and Gas Prospect Wells Drilled in California*, 258 pp., Calif. Dep. of Conserv., Sacramento.

Carena, S., and J. Suppe (2002), 3D imaging of active structures using earthquake aftershocks: The Northridge thrust, *J. Struct. Geol.*, *24*, 887–904.

Dibblee, T. W. (1971), Geologic maps of the Coalinga, Joaquin Rocks, New Idria, and Priest Valley 15-minute quadrangles, California, scale 1:62,500, *U. S. Geol. Surv. Open File*, *71–87*.

Dickinson, W. R. (2002), Reappraisal of hypothetical Franciscan thrust wedging at Coalinga: Implications for tectonic relations along the Great Valley flank of the California Coast Ranges, *Tectonics*, *21*(5), 1039, doi:10.1029/2001TC001315.

Dolan, J. F., S. A. Christofferson, and J. H. Shaw (2003), Recognition of Paleoearthquakes on the Puente Hills Blind Thrust Fault, California, *Science*, *300*, 115–118.

Eaton, J. P. (1990), The earthquake and its aftershocks from May 2 through September 30, 1983, in *The Coalinga, California Earthquake of May 2, 1983*, edited by M. Rymer and W. Ellsworth, *U. S. Geol. Surv. Prof. Pap.*, *1487*, pp. 113–170.

Eberhart-Phillips, D. (1989), Active faulting and deformation of the Coalinga anticline from three-dimensional velocity structure and seismicity, *J. Geophys. Res.*, *94*, 15,565–15,586.

Eberhart-Phillips, D. M., and P. A. Reasenberg (1990), Complex faulting structure inferred from local seismic observations of $M \geq 1.0$ aftershocks, May 2–June 30, 1983, in *The Coalinga, California Earthquake of May 2, 1983*, edited by M. Rymer and W. Ellsworth, *U. S. Geol. Surv. Prof. Pap.*, *1487*, 171–192.

Ekström, G., R. S. Stein, J. P. Eaton, and D. Eberhart-Phillips (1992), Seismicity and geometry of a 110-km-long blind thrust fault, 1. The 1985 Kettleman Hills, California earthquake, *J. Geophys. Res.*, *97*, 4843–4864.

Erickson, S. G. (1995), Mechanics of triangle zones and passive-roof duplexes: Implications of finite-element models, *Tectonophysics*, *254*, 1–11.

Erslev, E. A. (1991), Trishear fault-propagation folding, *Geology*, *19*(6), 617–620.

Fielding, E., M. Barazangi, L. Brown, J. Oliver, and S. Kaufman (1984), COCORP seismic profiles near Coalinga, California: Subsurface structure of the western Great Valley, *Geology*, *12*, 268–273.

Guzofski, C. A., J. H. Shaw (2005), Coalinga anticline, San Joaquin basin, California, U.S.A., in *Seismic Interpretation of Contractional Fault-*

Related Folds: An AAPG Seismic Atlas, edited by J. H. Shaw, C. Connors and J. Suppe, *AAPG Stud. Geol.*, 53, 138–140.

Hill, M. L. (1984), Earthquakes and folding, Coalinga, California, *Geology*, *12*, 711–712.

Lin, G., and P. Shearer (2005), Tests of relative earthquake location techniques using synthetic data, *J. Geophys. Res.*, *110*, B04304, doi:10.1029/2004JB003380.

Lin, J., and R. S. Stein (2004), Stress triggering in thrust and subduction earthquakes and stress interaction between the southern San Andreas and nearby thrust and strike-slip faults, *J. Geophys. Res.*, *109*, B02303, doi:10.1029/2003JB002607.

Mahrer, K. D., and A. Nur (1979), Static strike-slip faulting in a horizontally varying crust, *Bull. Seismol. Soc. Am.*, *69*, 975–1009.

Mansfield, C. F. (1991), Lithofacies and petrofacies map of upper Mesozoic rocks near Coalinga in the southern Diablo Range, California, *Oil Gas Invest. Map, Rep., OM-0221*.

McGarr, A., C. Mueller, J. B. Fletcher, and M. Andrews (1990), Ground-motion and source parameters of the Coalinga earthquake sequence, in *The Coalinga, California Earthquake of May 2, 1983*, edited by M. Rymer and W. Ellsworth, *U. S. Geol. Surv. Prof. Pap.*, *1487*, 215–234.

Medwedeff, D. A. (1989), Growth fault-bend folding at southeast Lost Hills, San Joaquin Valley, California, *AAPG Bull.*, *73*, 54–67.

Medwedeff, D. A. (1992), Geometry and kinematics of an active, laterally propagating wedge thrust, Wheeler Ridge, California, in *Structural Geology of Fold and Thrust Belts*, edited by S. Mitra and G. Fisher, pp. 3–28, John Hopkins Univ. Press, Baltimore, Md.

Meltzer, A. (1989), Crustal structure and tectonic evolution: Central California, Ph.D. thesis, Rice Univ., Houston Tex.

Michael, A. J. (1987), Stress rotation during the Coalinga aftershock sequence, *J. Geophys. Res.*, *92*, 7963–7979.

Mount, V. S., and J. Suppe (1987), State of stress near the San Andreas fault: Implications for wrench tectonics, *Geology*, *15*, 1143–1146.

Mueller, K., J. Champion, M. Guccione, and K. I. Kelson (1999), Fault slip rates in the modern New Madrid Seismic Zone, *Science*, *286*, 1135–1138.

Murray, J. R., P. Segall, P. Cervelli, W. Prescott, and J. Svarc (2001), Inversion of GPS data for spatially variable slip-rate on the San Andreas Fault near Parkfield, CA, *Geophys. Res. Lett.*, *28*(2), 359–362.

Namson, J., and T. L. Davis (1988), Seismically active fold and thrust belt in the San Joaquin Valley, central California, *Geol. Soc. Am. Bull.*, *100*, 257–273.

Namson, J. S., T. L. Davis, and M. B. Lagoe (1990), Tectonic history and thrust-fold deformation style of seismically active structures near Coalinga, in *The Coalinga, California Earthquake of May 2, 1983*, edited by M. Rymer and W. Ellsworth, *U. S. Geol. Surv. Prof. Pap.*, *1487*, 79–96.

Popovich, D. A., and K. C. Miller (2002), Crustal structure near Coalinga, California revisited: Implications for the hypocentral region of the 1983 M_L 6.7 earthquake, in *Eos Trans. AGU*, *83*(47), Fall Meet. Suppl., Abstract S11B-1151.

Richards-Dinger, K. B., and P. M. Shearer (2000), Earthquake locations in southern California obtained using source-specific station terms, *J. Geophys. Res.*, *105*(B5), 10,939–10,960.

Rubin, A. M., and D. Gillard (2000), Aftershock asymmetry/rupture directivity among central San Andreas fault microearthquakes, *J. Geophys. Res.*, *105*, 19,095–19,110.

Rybicki, K. (1978), Static deformation of a laterally inhomogeneous half-space by a two-dimensional strike-slip fault, *J. Phys. Earth*, *26*, 351–366.

Shaw, J., and P. Shearer (1999), An elusive blind thrust fault beneath metropolitan Los Angeles, *Science*, *283*, 1516–1518.

Shaw, J., and J. Suppe (1994), Active faulting and growth folding in the eastern Santa Barbara Channel, California, *Geol. Soc. Am. Bull.*, *106*, 607–626.

Shaw, J. H., C. Connors, and J. Suppe (Eds.) (2005), *Seismic Interpretation of Contractional Fault-Related Folds*: *An AAPG Seismic Atlas*, *AAPG Stud. Geol., 53*.

Shearer, P., E. Hauksson, and G. Lin (2005), Southern California hypocenter relocation with waveform cross-correlation, part 2: Results using source-specific station terms and cluster analysis, *Bull. Seismol. Soc. Am.*, *95*, 904–915, doi:10.1785/0120040168.

Shearer, P. M. (1997), Improving earthquake locations using L1 norm and waveform cross correlation: Application to the Whittier Narrows, California, aftershock sequence, *J. Geophys. Res.*, *102*, 8269–8283.

Stein, R. S., and G. Ekström (1992), Sesmicity and geometry of a 110-km-long blind thrust fault: 2. Synthesis of the 1982–1985 California earthquake sequence, *J. Geophys. Res.*, *97*, 4865–4883.

Stein, R. S., and G. C.P. King (1984), Seismic potential revealed by surface folding: 1983 Coalinga, California, earthquake, *Science*, *224*, 869–872.

Strayer, L., and J. Suppe (2002), Out-of-plane motion of a thrust sheet during along-strike propagation of a thrust ramp: A distinct-element approach, *J. Struct. Geol.*, *24*, 637–650.

Suppe, J. (1983), Geometry and kinematics of fault-bend folding, *Am. J. Sci.*, *283*, 684–721.

Suppe, J., and D. A. Medwedeff (1990), Geometry and kinematics of fault-propagation folding, *Ecologae Geol. Helv.*, *83*(3), 409–454.

Suppe, J., F. Sàbat, J. A. Munoz, J. Poblet, E. Roca, and J. Vergés (1997), Bed-by-bed fold growth by kink-band migration: Sant Llorenç de Morunys, eastern Pyrenees, *J. Struct. Geol.*, *19*(3–4), 443–461.

Suppe, J., Y. H. Lee, Y. G. Chen, and J. H. Hung (2000), Coseismic fault-bend folding: fold scarp formation in the 199 Chi-Chi Earthquake (M 7.6), Taiwan Fold-and-Thrust Belt, *Eos Trans. AGU*, *81*(48), Fall Meet. Suppl., Abstract S71E-09.

Suppe, J., C. C. Connors, Y. Zhang (2005), Shear Fault-Bend Folding, in *Thrust Tectonics and Hydrocarbon Systems*, edited by K. R. Mcclay, *AAPG Mem.*, *82*, 303–323.

Thatcher, W., and T. Hanks (1973), Source parameters of southern California earthquakes, *J. Geophys. Res.*, *78*, 8547–8576.

Walter, A. (1990), Upper-crustal velocity structure near Coalinga, as determined from seismic refraction data, in *The Coalinga, California Earthquake of May 2, 1983*, edited by M. Rymer and W. Ellsworth, *U. S. Geol. Surv. Prof. Pap.*, *1487*, 23–39.

Wentworth, C. M., and M. D. Zoback (1989), The style of late Cenezoic deformation at the eastern front of the California coast ranges, *Tectonics*, *8*, 237–246.

Wentworth, C. M., and M. D. Zoback (1990), Structure of the Coalinga area and thrust origin of the earthquake, in *The Coalinga, California Earthquake of May 2, 1983*, edited by M. Rymer and W. Ellsworth, *U. S. Geol. Surv. Prof. Pap.*, *1487*, 41–68.

Wessel, P., and W. H. F. Smith (1991), Free software helps map and display data, *Eos Trans. AGU*, *72*, 441.

Zoback, M., et al. (1988), New evidence on the state of stress of the San Andreas fault system, *Science*, *238*, 1105–1111.

C. A. Guzofski, Chevron ETC, 1500 Louisiana Street, Houston, TX 77002, USA.(guzofski@chevron.com)

G. Lin and P. M. Shearer, Institute of Geophysics and Planetary Physics, Scripps Institution of Oceanography, University of California, San Diego, La Jolla, CA 92093, USA.

J. H. Shaw, Department of Earth and Planetary Sciences, Harvard University, 20 Oxford Street, Cambridge, MA 02138, USA.